Peptide	Sequence	Average Hydro-phobicity (*H*)[2]	Average Hydro-phobicity (*H*)[1]	Angle	Hydrophobic moment* (μ*H*)[1]
D-LAK60	*KKLAL**K**ALLLWL**K**ALL**K**LA**K**LALKK*	-0.05	1.26	60	2.28
D-LAK80	*KKLAL**K**AL**K**LWLLALL**K**LA**K**LALKK*	-0.05	1.26	80	1.95
D-LAK100	*KKLAL**K**AL**K**LWLLAL**KK**LALLALKK*	-0.05	1.26	100	1.56
D-LAK120	*KKLALLAL**KK**WLLAL**KK**LALLALKK*	-0.05	1.26	120	1.28
D-LAK140	*KKLA**K**LALL**K**WLLAL**KK**LALLALKK*	-0.05	1.26	140	0.76
D-LAK160	*KKLA**K**LALL**K**WLLAL**K**LLAL**K**ALKK*	-0.05	1.26	160	0.51

Supplementary Table 1. Comparison of physical features of peptides used in this study. Hydrophobicity (H) and mean hydrophobic moment (μH) are shown according to the Combined Consensus scale[1] or Eisenberg scale[2] and were calculated using the HydroMCalc Java applet made available by Alex Tossi (http://www.bbcm.univ.trieste.it/~tossi/HydroCalc/HydroMCalc.html).
All peptides contain eight lysine residues and are amidated at the C-terminus conferring a nominal charge of +9 at neutral pH. * Mean hydrophobic moment assuming formation of ideal α-helix.

	MIC50 (μM)		
Peptide	*E. coli* (NCTC 9001)	*P. aeruginosa*	*E. coli* (Top 10)
D-LAK60	> 22.62	> 22.62	7.07 ± 2.04
D-LAK80	> 22.62	> 22.62	5.40 ± 1.01
D-LAK100	4.14 ± 1.03	7.92 ± 2.06	1.51 ± 0.23
D-LAK120	1.48 ± 0.53	2.71 ± 1.07	0.62 ± 0.15
D-LAK140	3.14 ± 1.28	4.69 ± 0.67	0.76 ± 0.18
D-LAK160	3.85 ± 0.64	6.23 ± 0.71	1.49 ± 0.56

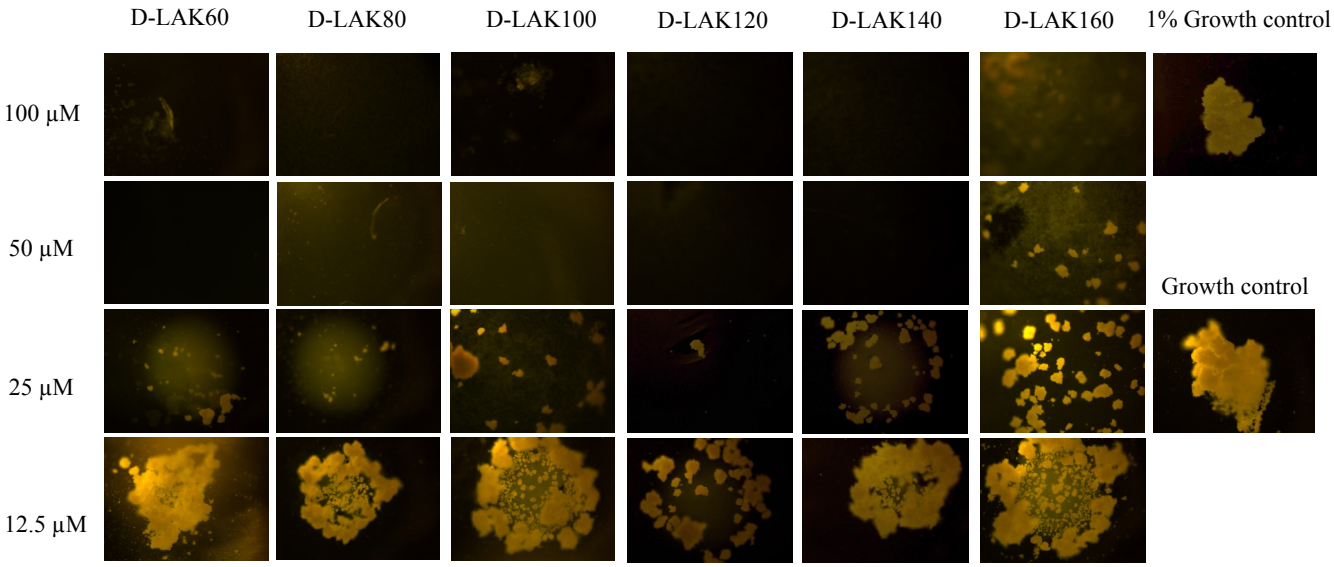

Supplementary Table 2/Figure 1. Comparison of antibacterial activities for the D-peptide angle variation series (Supp. Tab. 1). The optimal activity against all three Gram negative bacterial strains and also *M. tuberculosis* was obtained with peptide analogue where the angle subtended by the four lysine residues distributed in the centre of the peptide is 120°.

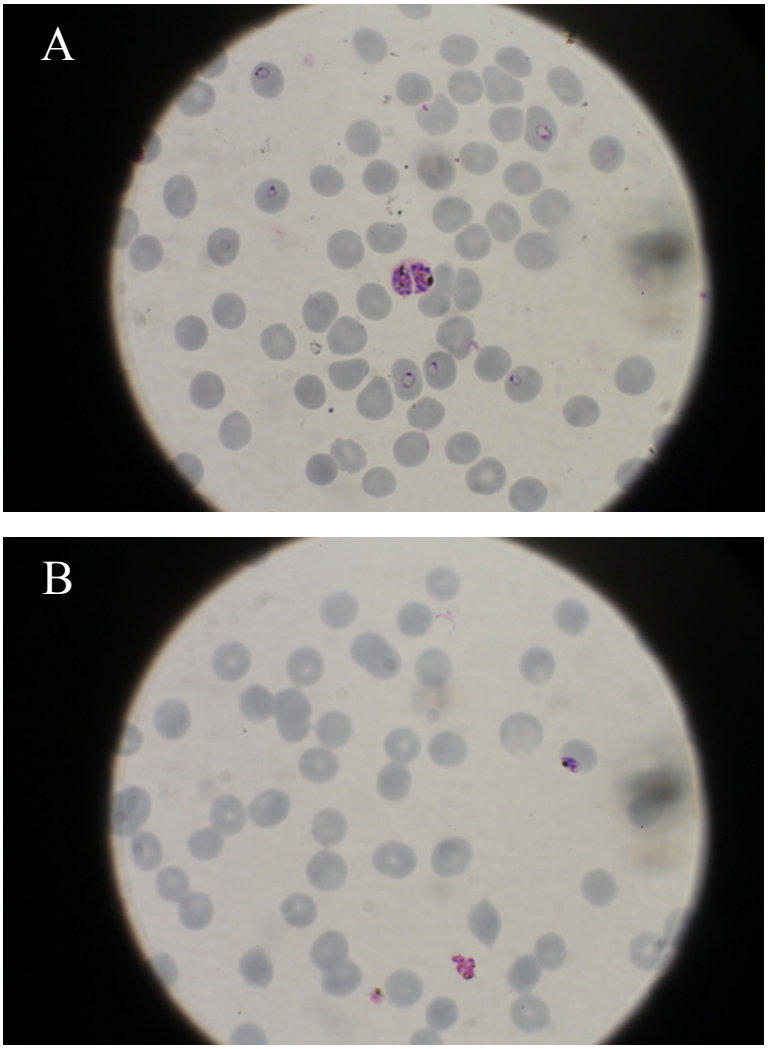

Supplementary Figure 2. Comparison of the effect of differing concentrations of D-LAK120-AP13 on erythrocyte stages of *Plasmodium falciparum* (3D7) observed using light microscopy. At sub-inhibitory concentrations (0.18 μM) a large number of early trophozoite or ring stage parasites can be seen along with a doubly schizont infected cell in the centre of the field (A). At inhibitory concentrations of the peptide (2.9 μM), red blood cells can be seen to be intact and largely devoid of parasitemia; the parasites appear grossly abnormal and probably non-viable (B).

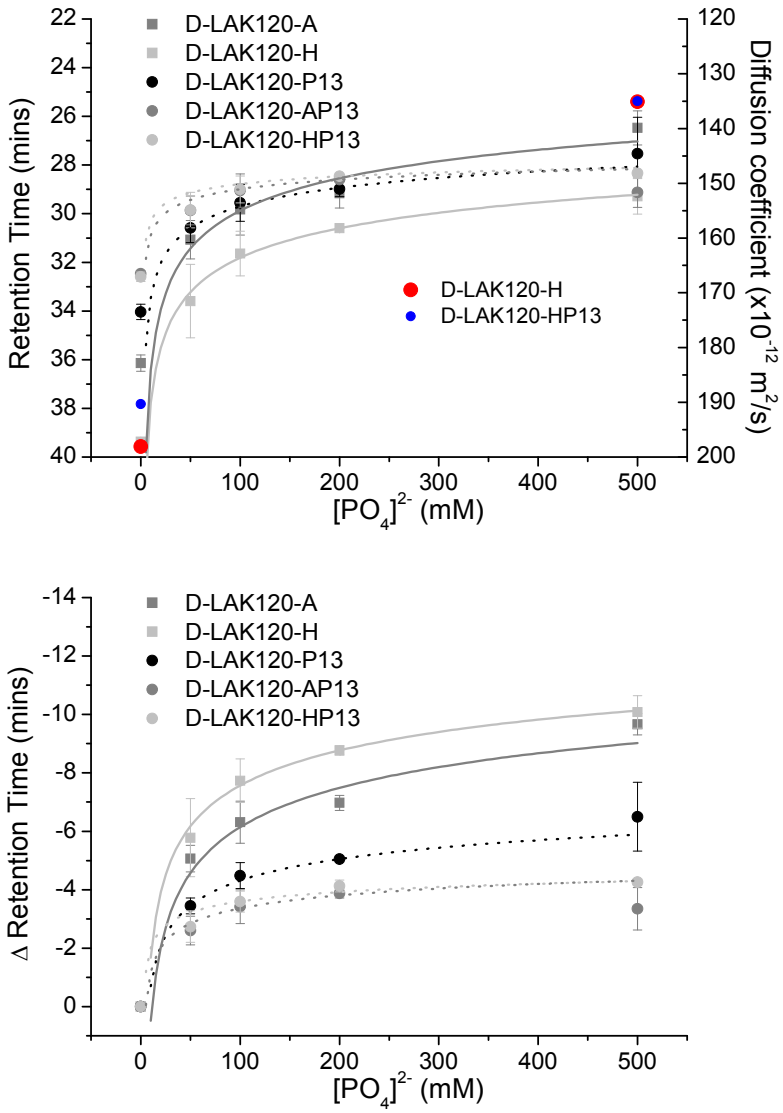

Supplementary Figure 3. Comparison of the absolute retention times (top) for the D-LAK peptides in the size exclusion chromatography experiment (grayscale) with diffusion coefficients determined by NMR spectroscopy (colour). Assuming absolute retention time and diffusion coefficients can be directly correlated to particle size, the proline containing peptides form larger particles at low phosphate concentrations when compared with proline free peptides. Increasing concentrations of phosphate anion increase the retention time and slow the diffusion of the peptides. At high phosphate concentrations, both techniques indicate the particles formed of either proline free or proline containing peptides are of very similar sizes.

Similar results were obtained for LAK120/LAK120-P10 using DOSY. In 500 mM $[PO_4]^{2-}$ the peptides had similar diffusion coefficients of 151.0 and 154.1 × 10^{-12} m^2/s for LAK120 and LAK120-P10 respectively. At 0 mM $[PO_4]^{2-}$, as with the D-peptides above, a more substantial difference was again noted with coefficients of 201.2 × 10^{-12} m^2/s for LAK120 comparing with 183.9 × 10^{-12} m^2/s for LAK120-P10.

The comparison based on relative retention times (Fig. 2D) is reproduced below for comparison.

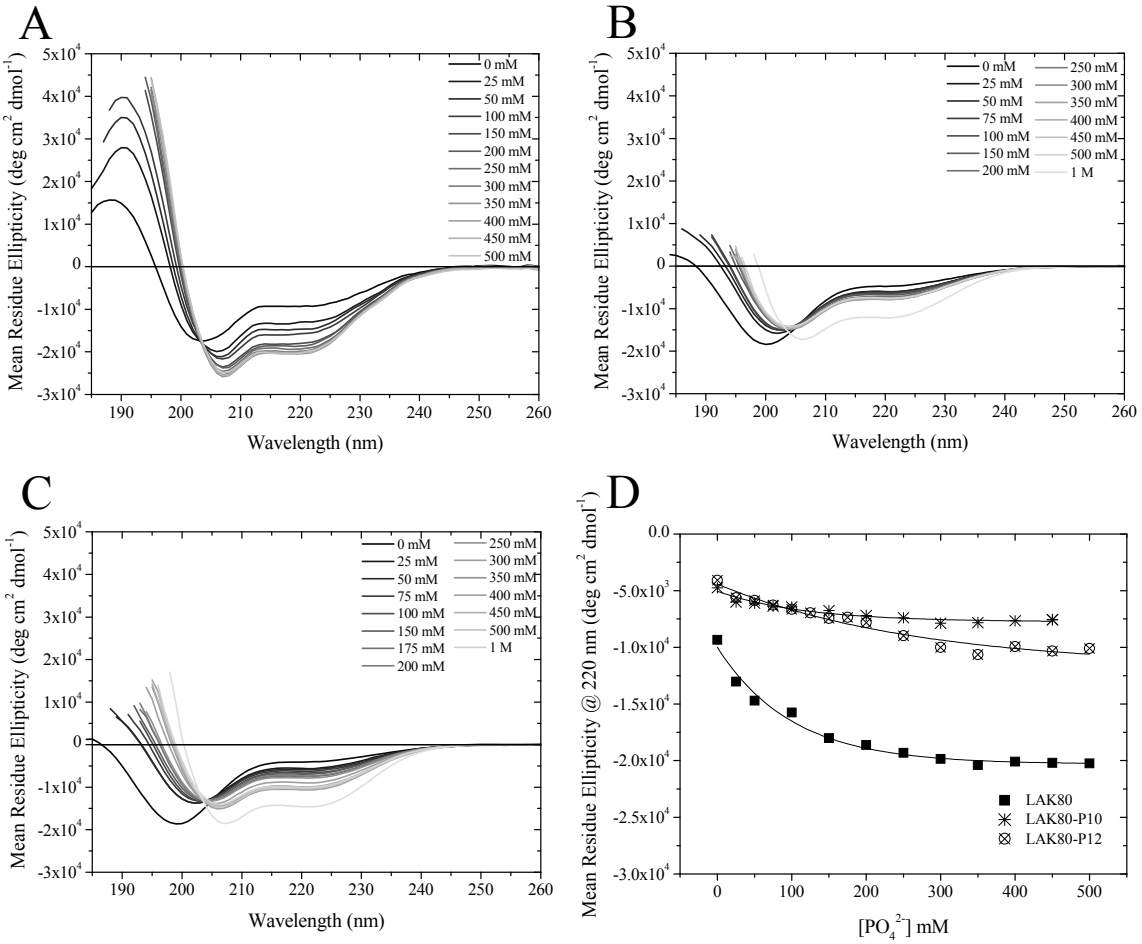

Supplementary Figure 4. Circular dichroism spectra of LAK80 (**A**), LAK80-P10 (**B**) and LAK80-P12 (**C**) in 5mM Tris buffer solution titrated with increasing concentrations of phosphate buffer at 37°C. The changes in α-helix content as monitored by the ellipticity at 220 nm is shown as a function of phosphate concentration (**D**).

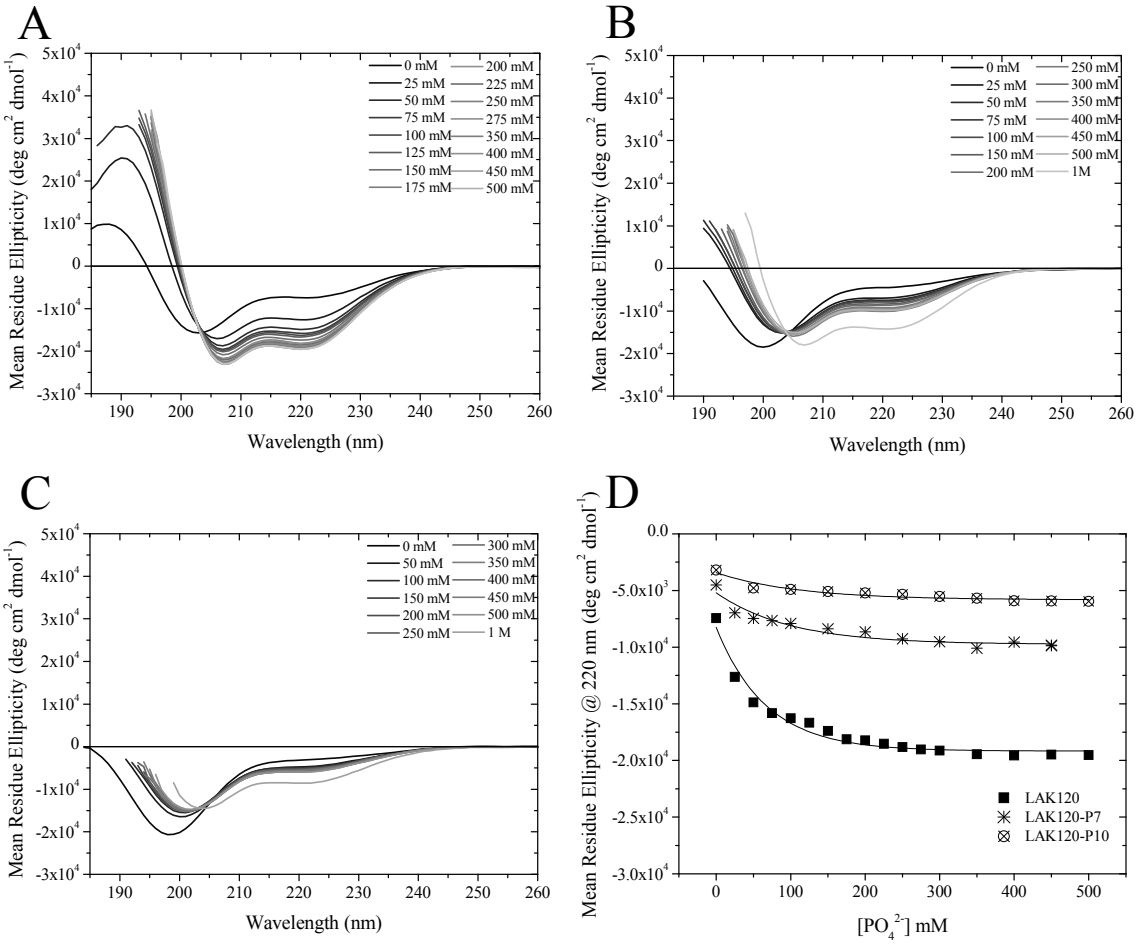

Supplementary Figure 5. Circular dichroism spectra of LAK120 (**A**), LAK120-P7 (**B**) and LAK120-P10 (**C**) in 5mM Tris buffer solution titrated with increasing concentrations of phosphate buffer at 37°C. The changes in α-helix content as monitored by the ellipticity at 220 nm is shown as a function of phosphate concentration (**D**).

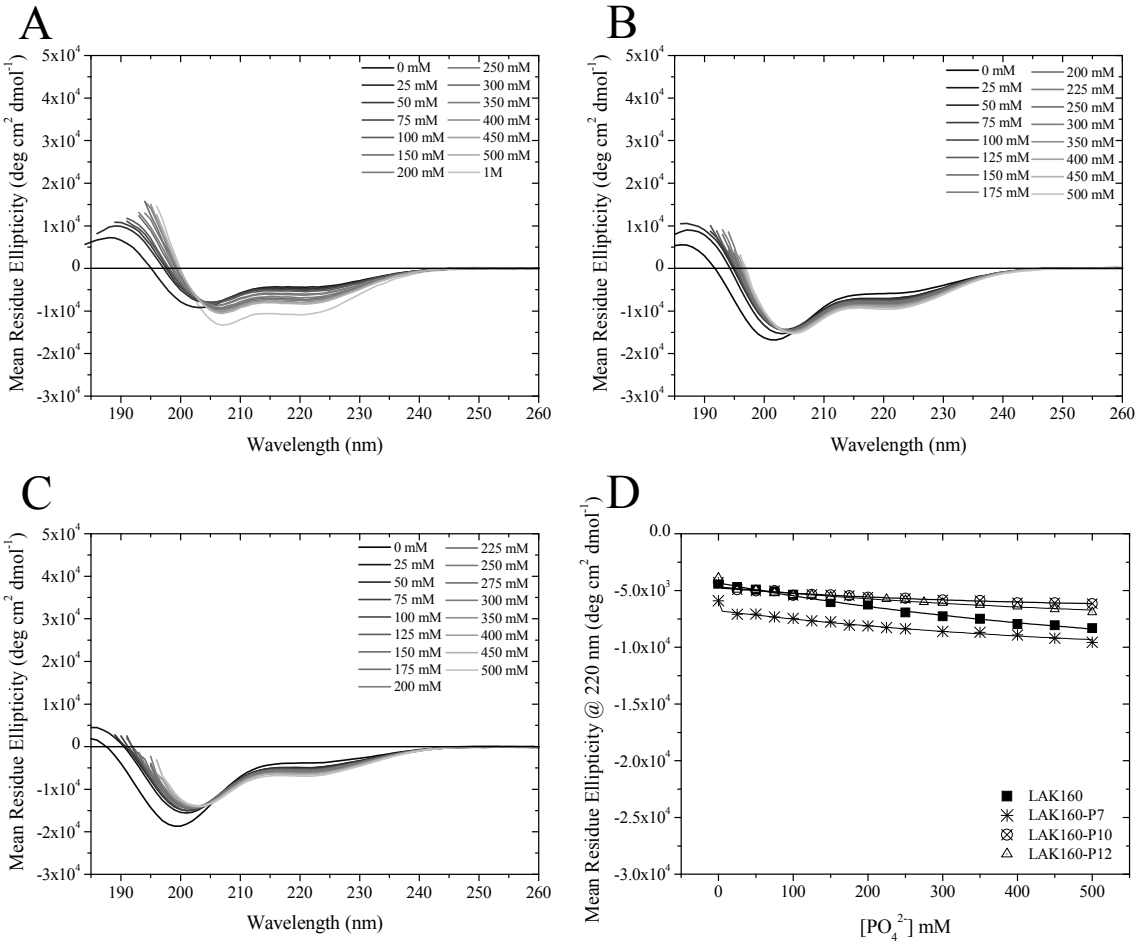

Suplpementary Figure 6. Circular dichroism spectra of LAK160 (**A**), LAK160-P7 (**B**) and LAK160-P12 (**C**) in 5mM Tris buffer solution titrated with increasing concentrations of phosphate buffer at 37°C. The changes in α-helix content as monitored by the ellipticity at 220 nm is shown as a function of phosphate concentration (**D**).

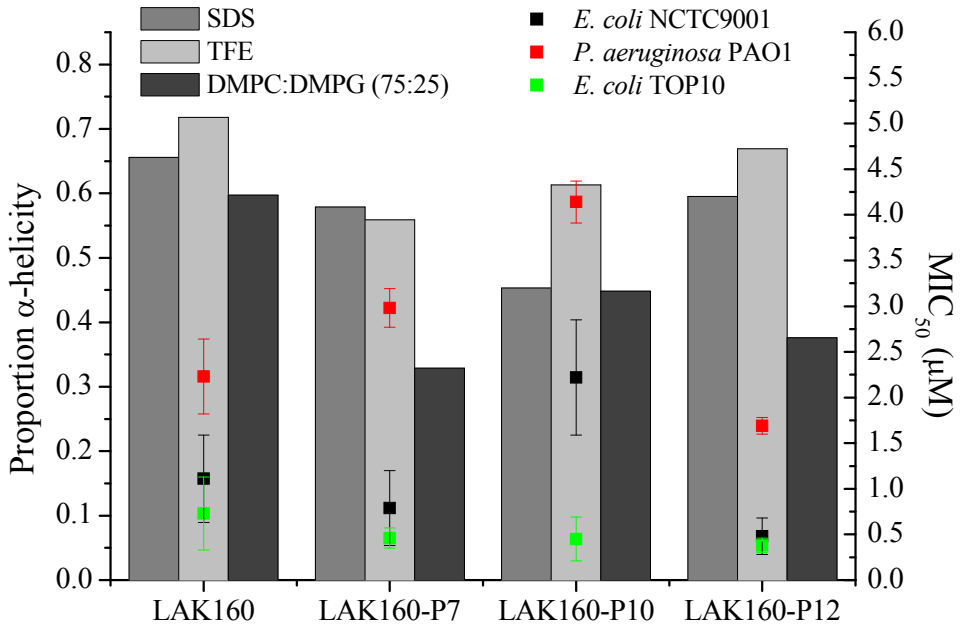

Supplementary Figure 7. Circular dichroism analysis of LAK160, LAK160-P7, LAK160-P10 and LAK160-P12 in a variety of membrane mimicking media. The environmental dependent changes in α-helix content as monitored by CDPro analysis of the whole spectral region are compared with the MIC50 obtained for three Gram-negative bacteria. Incorporation of proline at position 10 in the LAK160 sequence impairs the antibacterial function. In contrast, when incorporated at position 7 or 12, proline may significantly increase the antibacterial potency. Of the 3 proline containing LAK160 peptides, LAK160-P10 has the lowest α-helix content in the presence of 50 mM SDS but the greatest α-helix content in the presence of DMPC:DMPG (75:25) liposomes. When *E. coli* TOP10, which has deficient LPS, is challenged, much less variation in MIC is observed.

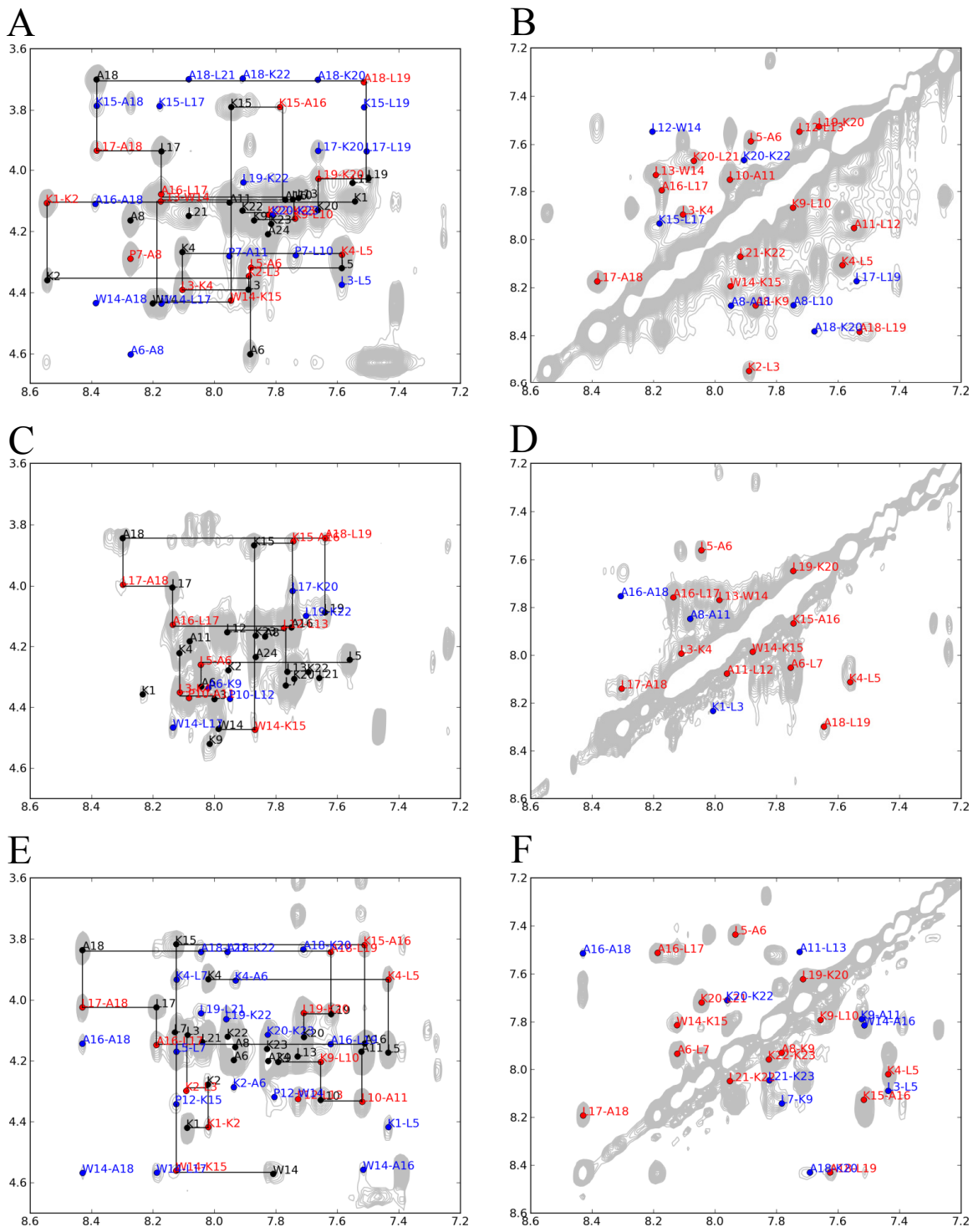

Supplementary Figure 8. NOESY spectra acquired for LAK160 proline containing peptides in the presence of 50 mM SDS at 310K at 500 MHz for ^{1}H. The H_{α}-H fingerprint region (**A**, **C**, **E**) and H-H contacts (**B**, **D**, **F**) are shown for LAK160-P7 (**A**, **B**), LAK160-P10 (**C**, **D**) and LAK160-P12 (**E**, **F**). Some H-H assignments are shown on the bottom right of the diagonal but, for structure calculations only peaks above the diagonal were integrated and used. ^{1}H NOESY spectra were recorded for each of the three LAK160 peptides in the presence of 50 mM SDS. The chemical shift dispersion of the Hα protons is similar for all three peptides, while the dispersion of NH protons is markedly smaller for LAK160-P10, possibly indicating a less structured peptide. H-H contacts are indicative of a helical structure, and it can be seen that fewer such contacts are present for LAK160-P10. Black annotation is used for intra-residue contacts, red for sequential contacts and blue for non-sequential contacts. Full peak assignments are available from the BMRB.

	LAK160-P7	LAK160-P10	LAK160-P12
Assignments used	82	61	81
Violations	0	0	0
Intra residue	23	23	23
Sequential	35	25	30
Short range (2-3Å)	20	13	23
Medium range (4-5Å)	4	0	5
Long range (>5Å)	0	0	0
Average energy (stdev)	-612 (48)	-559 (45)	-602 (40)
Favored dihedrals	61%	60%	58%
Allowed dihedrals	35%	34%	37%
Generously allowed	2%	5%	2%
Disallowed	1%	1%	2%
Region 1 (RMSD)	5-12 (0.95)	5-11 (0.89)	2-9 (0.93)
Region 2 (RMSD)	13-23 (0.95)	14-19 (0.94)	14-22 (0.95)
Proportion α-helix (CD)	0.58	0.45	0.60

Supplementary Table 3. Results and statistics of structure calculations with backbone atoms (H_α and H) and PRO-H_δ protons only. Violations and energies are given as reported by the ARIA software. The allowed regions for the backbone dihedral angles are given as reported by the procheck_nmr software. Also given are regions of the peptides that can be used to align the peptides giving the lowest average RMSD. A large number of backbone contacts have been assigned, and structures could be calculated without a single violation. Energies of the resulting structures are low. The structure of a 24-residue peptide is considered as converged when it has an energy lower than 240 kcal mol-1. A variation of less than 10% is considered normal. Around 95% of all dihedral angles are in the favoured or allowed regions for all three structures, indicating that the NOE restraints do not lead to unfavourable or disallowed conformations.

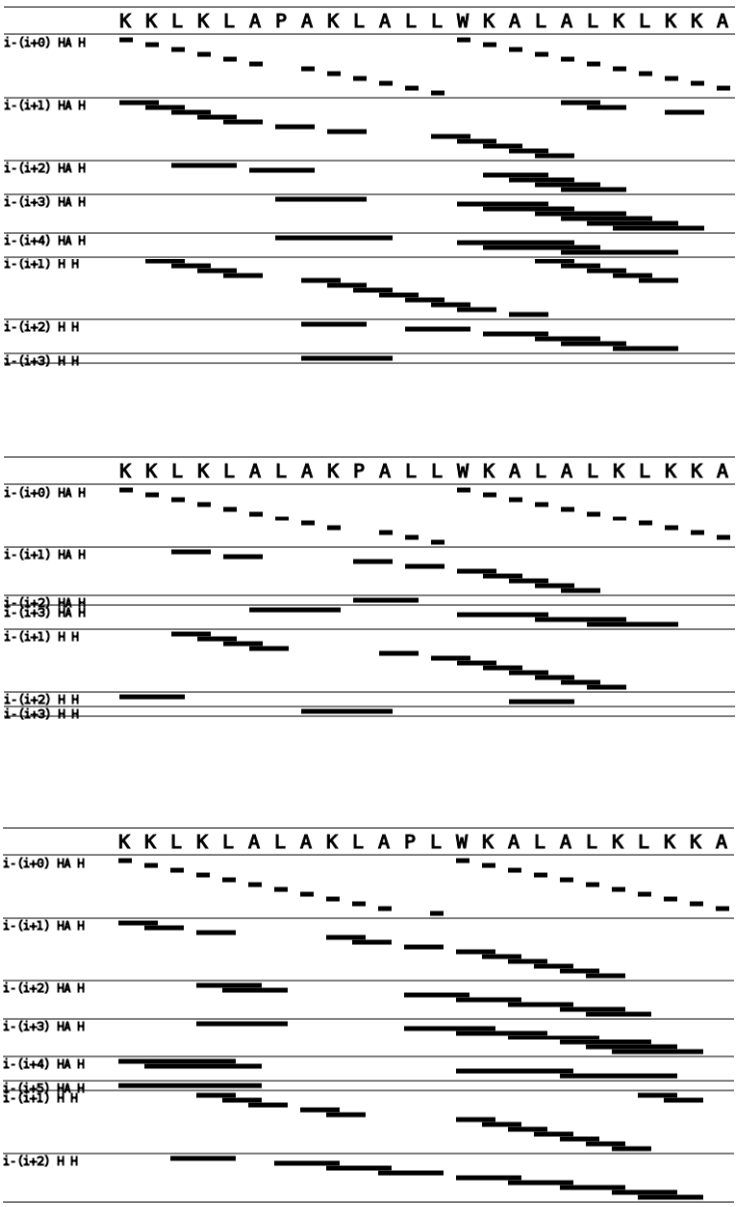

Supplementary Figure 9. Overview of NOE connectivites for LAK160-P7 (top), LAK160-P10 (middle) and LAK160-P12 (bottom).

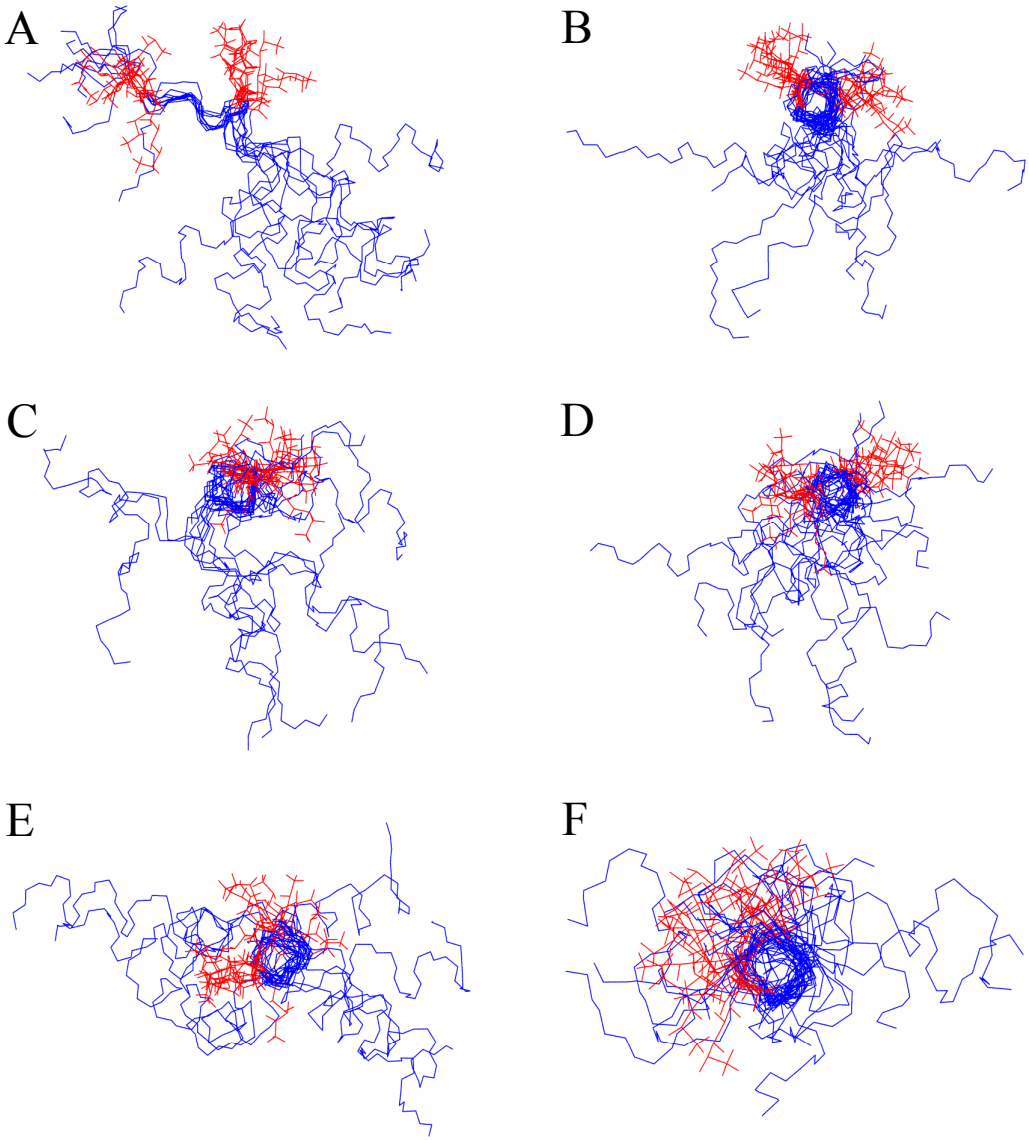

Supplementary Figure 10. Angle between lysine 4 and 9 (**A**, **C**, **E**) and lysine 15 and 20 (b, d, f) after fitting the backbone residues as given in table 2. The side chains of the lysine residues are shown in red, the trace of the backbone of the rest of the peptide is shown in blue. α-helix segments of the peptide were manually aligned so their helix axis is perpendicular to the viewing plane. In (**A**), where no helical structure is observed, a representation is chosen that most clearly represents the situation. In (**C**), although this structure is not recognised as α-helical, an axis running through the fitted region of the peptide can be defined and is shown perpendicular to the viewing plane. Panels (**B**), (**D**), and (**F**) are viewed from the C-terminus while panels (**C**) and (**E**) viewed from the N-terminus.